iScience

CellPress
OPEN ACCESS

Article

Spontaneous water oozing of a soft drain bed via energy-free atmospheric water harvesting

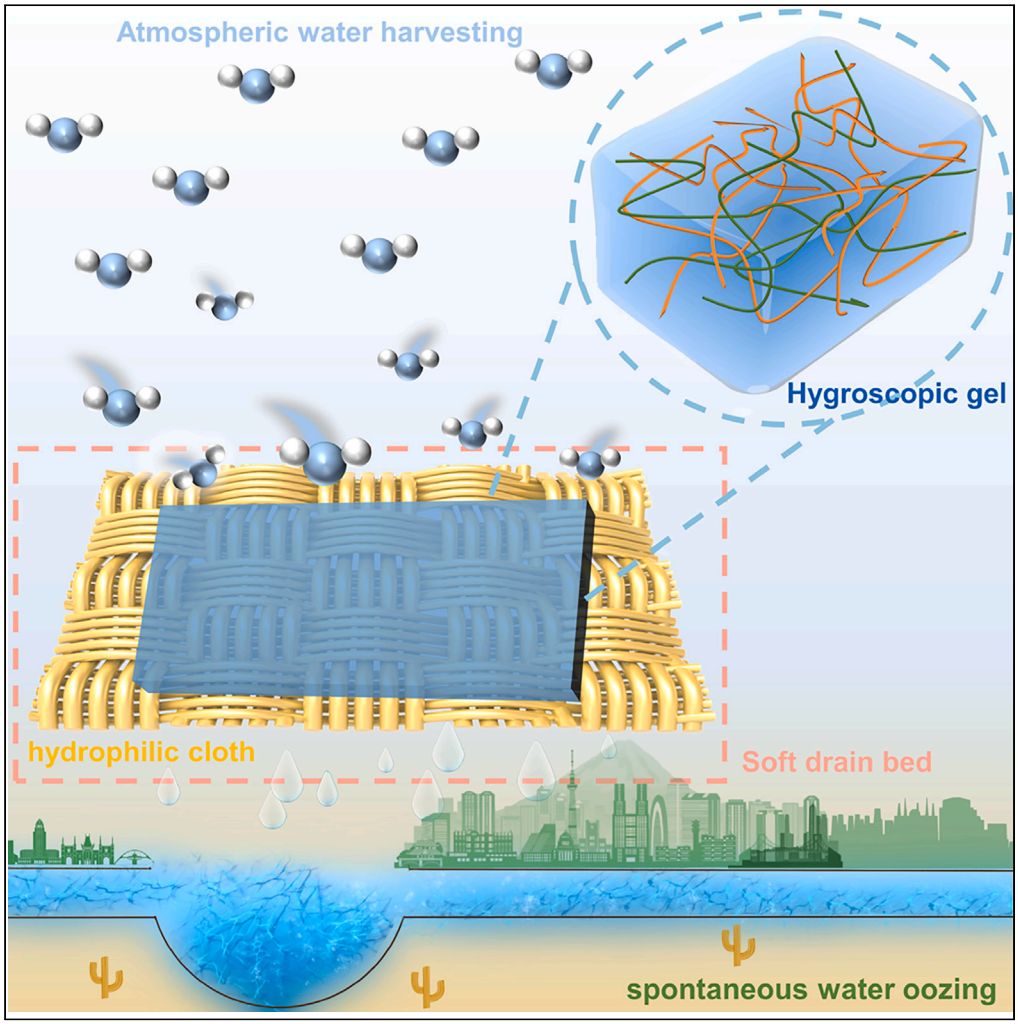

Yang-Hui Luo, Xue-Ting Jin, Min Liu, Si-Wei Sun, Jie Zhao

luoyh2016@seu.edu.cn

Highlights

A soft drain bed for spontaneous water oozing has been fabricated

The spontaneous water oozing can be performed under all-weather humidity conditions

The high potential for practical freshwater supply application has been demonstrated

Luo et al., iScience 27, 110492
August 16, 2024
https://doi.org/10.1016/j.isci.2024.110492

iScience

CellPress
OPEN ACCESS

Article

Spontaneous water oozing of a soft drain bed via energy-free atmospheric water harvesting

Yang-Hui Luo,[1,2,*] Xue-Ting Jin,[1] Min Liu,[1] Si-Wei Sun,[1] and Jie Zhao[1]

SUMMARY

Atmospheric water harvesting has emerged as an efficient strategy for addressing the global challenge of freshwater scarcity. However, the in being energy-consuming water-collecting process has obstructed its practicality. In this work, a soft drain bed, which was composed of hydrophilic cloth and hygroscopic gel, has been demonstrated to capture atmospheric water effectively, followed by converting it into liquid water spontaneously and sustainably, under all-weather humidity conditions. Under the optimal working condition of 30°C with a relative humidity level of 75%, the bed can provide a spontaneous water oozing ability of 1.25 g $_{(liquid\ water)}$/hour within the 8 h of working time. More importantly, after 5 working cycles, 80% of the oozing ability can be reserved, suggesting the high potential for practical freshwater supply application. The proposed design strategy is expected to provide new hints for the development of future energy-saving decentralized freshwater supply systems.

INTRODUCTION

Water is the cradle of human life.[1,2] Sufficient freshwater is conducive to the physical and mental health of the country and its people, economic development, and environmental protection.[3,4] However, with the continuous development of the economy and the continuous growth of the population, the shortage of freshwater resources has become a serious challenge for the world.[5,6] Atmospheric water accounts for about 10% of the total freshwater resources in lakes on the Earth,[7–9] which is a very large treasure of fresh water, so the collection has become the focus of many researchers. The methods for atmospheric water collection mainly include three aspects: fog collection,[10–12] air cooling,[13] and atmospheric water harvesting (AWH) by using sorption materials.[14–17] Among them, fog collection is highly dependent on the geography and location, while air cooling requires areas with high humidity, and the accompanied condensers consume a lot of energy. Relatively, AWH technology is more promising, as it can eliminate the limitations on weather and region.[18–20]

However, till now, almost all of the developed AWH technologies are more or less energy intensive, as the release of the captured water needs the presence of such energy as heat,[21–23] solar energy,[24–26] electricity,[27] or magnetic fields,[28] and further condensation of the released vapor into liquid water is energy intensive as well.[29–31] As a consequence, energy consumption has become one of the main obstacles to the widespread application of AWH.[32–35] In this sense, the fabrication of appropriate material that can convert the captured vapor into liquid water, via spontaneous *in-situ* liquefaction, is expected to contribute significantly to the development of energy-free AWH technologies, which will earnestly promote the practical application of AWH for decentralized freshwater supply, as both the energy-intensive processes of water release and condensation have been left out.[36]

Here, in this work, we have fabricated a soft drain bed by using hydrophilic cloth and hygroscopic gel, which can capture atmospheric water effectively, followed by converting it into liquid water spontaneously (Scheme 1), under all-weather humidity conditions (relative humidity [RH] levels of 30%–98%) around room temperatures (20°C–35°C). Hanging the soft drain bed in the humid atmosphere has achieved spontaneous water oozing. Results revealed that, under 30°C conditions with an RH level of 75%, the soft drain bed with a volume of 9.8 cm^3 can collect 10 g of freshwater within optimal working time of 8 h, providing an energy-free spontaneous water oozing ability of 1.25 g/h. In addition, the soft drain bed can repeat the spontaneous water oozing process for at least 5 cycles, with only a 20% decrease in the capacity, and all the collected oozing water throughout the 5 cycles meets the World Health Organization (WHO) drinking water standards.[37] The present work is expected to provide new insight into the design of future energy-saving decentralized freshwater supply systems, and others.

RESULTS AND DISCUSSIONS

Preparation and characterization of soft drain bed

The soft drain bed was constructed by hydrophilic cloth coated with hygroscopic gel on both sides; the latter was composed of two-dimensional (2D) hygroscopic powder bridged through porous rigid hydrophobic polymer support (see the Method Details). The grid-like brown-colored hydrophilic cloth was provided by the Atmospheric Water Research Center (Qiandao Lake, Hangzhou, China) (Figure 1A), and it was

[1]School of Chemistry and Chemical Engineering, Southeast University, Nanjing 211189, P.R. China
[2]Lead contact
*Correspondence: luoyh2016@seu.edu.cn
https://doi.org/10.1016/j.isci.2024.110492

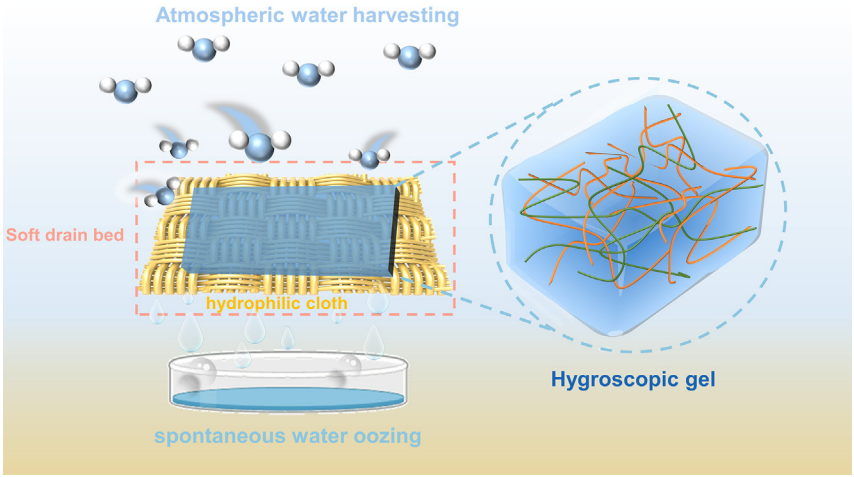

Scheme 1. Illustrating the composition and performance of the soft drain bed

weaved by using a polyvinyl alcohol line via electrospinning (Figure 1B). The ingredient of hygroscopic powder was hetero-layered 2D isomorphic metal-organic framework nanosheets (Figure 1C).[38] The porous rigid hydrophobic polymer support was hydrophobic polymer polyvinylidene fluoride (Figure 1D), with a small addition of polyethylene glycol.[39,40] To fabricate the soft drain bed, the prepared hygroscopic powder was first dispersed in the hydrophobic polymer support to form a blue-colored hygroscopic gel (Figure 1E); the latter was then coated on the two sides of the hydrophilic cloth and was followed by solidification. Note that, to achieve maximum exposure, the soft drain bed was molded into a cylindric-like motif (Figures 1F and S1). The scanning electron microscopy (SEM) image of sections suggested the firm adherence of the hygroscopic gel to the hydrophilic cloth (Figure 1G). Importantly, micron-sized pores were observed throughout the whole body of the drain bed (Figure 1H), which is expected to contribute significantly to the smooth pass in and out of both the gaseous and liquid water from the drain bed.[41]

Energy-free AWH

To evaluate its energy-free AWH ability, we put the soft drain bed in a glass dish with an inside diameter of 10 cm and exposed it to the atmosphere with an RH level of 60% under ambient conditions. The obvious color change from blue to gray can be observed on the drain bed within 30 min (Figure 2A), corresponding to its effective AWH.[39] More encouragingly, freshwater began to ooze from the drain bed spontaneously after extending the exposure time to 60 min, and the amount of the freshwater increased with the exposure time. We then performed ICP-MS and TOC for total organic carbon to evaluate the quality of the oozing water; results revealed that the concentrations of both the metal ions (Li^+, Na^+, K^+, Ga^{2+}, and Mg^{2+}) and TOC are lower than those of the WHO water quality standard (Figure 2B). In this sense, the goal of spontaneous water oozing can be expected on this soft drain bed.

The aforementioned encouraging aspect must be attributed to the special structure of the hygroscopic powder, as it was featured with an appropriate 1.0 nm pore diameter (Figure 2C), as well as sufficient density of adsorption sites of 34.6% (Figure 2D); these two data are approaches to the most desirable critical factors, ~1.0 nm pore size and ~40% density of adsorption sites, for achieving excellent AWH performance.[42] In addition, the 2D nature of the hygroscopic powder featured with large specific surface area, and rich hydrophilic active sites,[38] which is expected to reduce the water vapor pressure on the 2D surface; as a consequence, fast water absorption and liquefaction on the surfaces of hygroscopic powder are theoretically feasible.[41] In fact, the exposure to the atmosphere with an RH level of 60% for 24 h can change the solid-state blue-green-colored hygroscopic powder into a reddish-brown-colored water drop (Figure 2E). In addition, the water vapor sorption isotherms of hygroscopic powder resemble a typical type-III sorption curve (Figure 2F), indicating the weak interaction between the 2D surfaces and water, which must contribute extensively to the spontaneous water oozing.[41] The large capillary condensation hysteresis throughout the whole pressure region suggests the generation of new mesopores that can act as a warehouse for the storage of water clusters during the AWH process.[43] The AWH capacity of hygroscopic powder is found to be 1,377 mg g^{-1} (Figure 2F insert), a value among the most excellent adsorbents reported in the literature.[44] Meanwhile, X-ray photoelectron spectroscopy (XPS) indicated that the dispersion in the hydrophobic polymer support did not affect the structure of the hygroscopic powder (Figure 3A); in other words, the intrinsic energy-free AWH performance and spontaneous water oozing ability of hygroscopic powder were well preserved in the soft drain bed.

Spontaneous water oozing

To further investigate the influence of RH levels and temperatures on the spontaneous water oozing ability, the soft drain bed was hung in an inclosed incubator with controlled RH levels and temperatures (Figure S2), and a beaker was right under the bed to collect the spontaneously oozing water (Figure 3B). The RH levels and temperatures of the incubator were tuned from 30% to 98% and 20°C to 30°C, respectively. Results revealed that, under the lower RH levels of 30% and 45%, the hanging soft drain bed has shown excellent AWH ability accompanied by

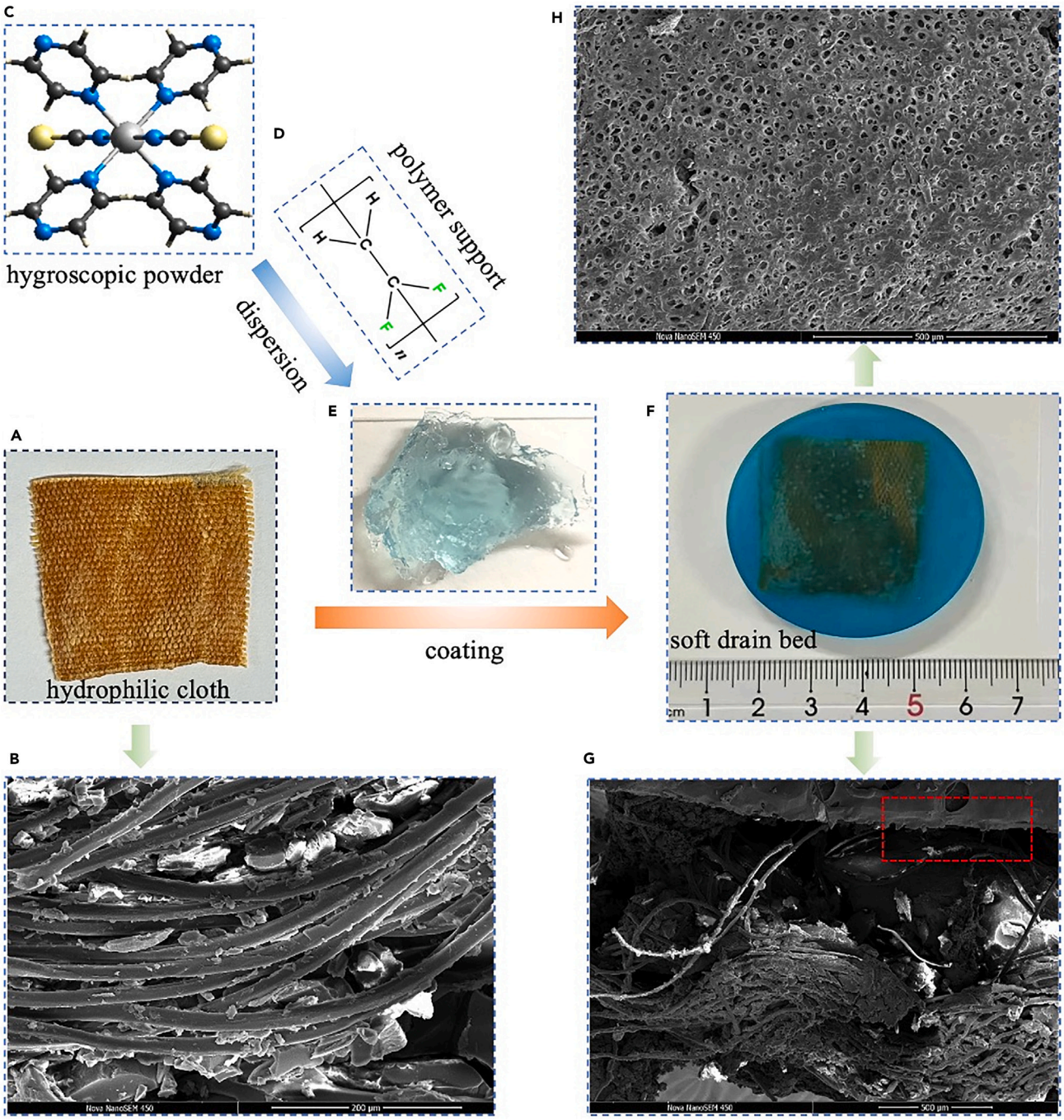

Figure 1. Fabrication and morphology characterization of the soft drain bed

(A) Digital images of the hydrophobic cloth.
(B) SEM images of the hydrophobic cloth.
(C) Molecular structure of hygroscopic powder.
(D) Molecular structure of polymer support.
(E) Digital images of hydrophobic gel.
(F) Digital images of soft drain bed.
(G) SEM images of section of soft drain bed.
(H) SEM images of surface of soft drain bed.

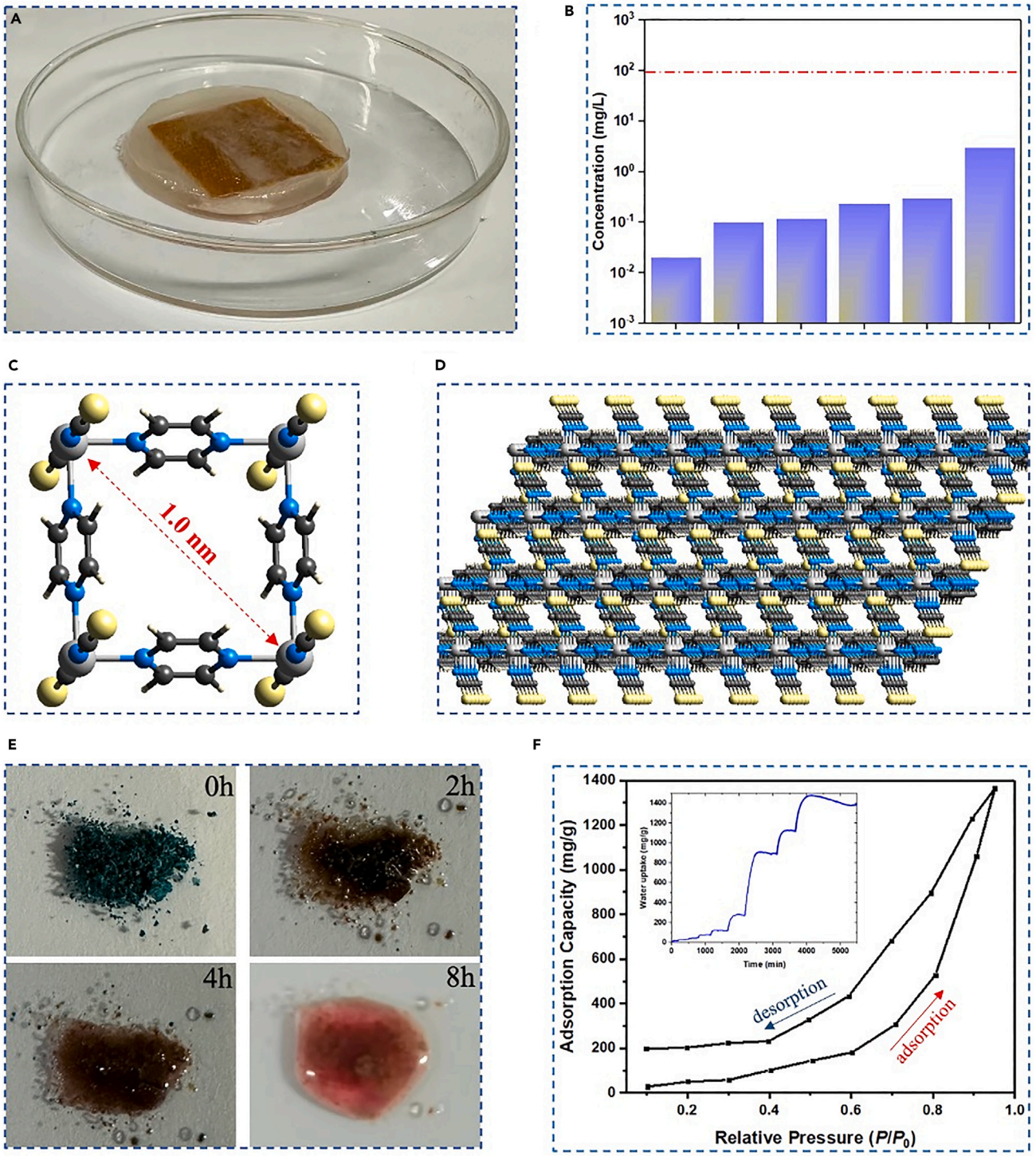

Figure 2. AWH performance of the soft drain bed

(A) Digital image of the soft drain bed after being exposed to a humid atmosphere for 1 h.

(B) ICP-MS and TOC analysis results of the spilled freshwater in (A), the concentrations of Li^+, Na^+, K^+, Ca^{2+}, Mg^{2+}, and TOC are all below the WHO drinking standard (see red dashed line).

(C) Pore size of the hygroscopic powder.

(D) Layered motif of the hygroscopic powder.

(E) Digital images of the hygroscopic powder exposed in a humid atmosphere with different times.

(F) Vapor sorption isotherm of the hygroscopic powder; inset was the time-dependent water uptake during the adsorption process.

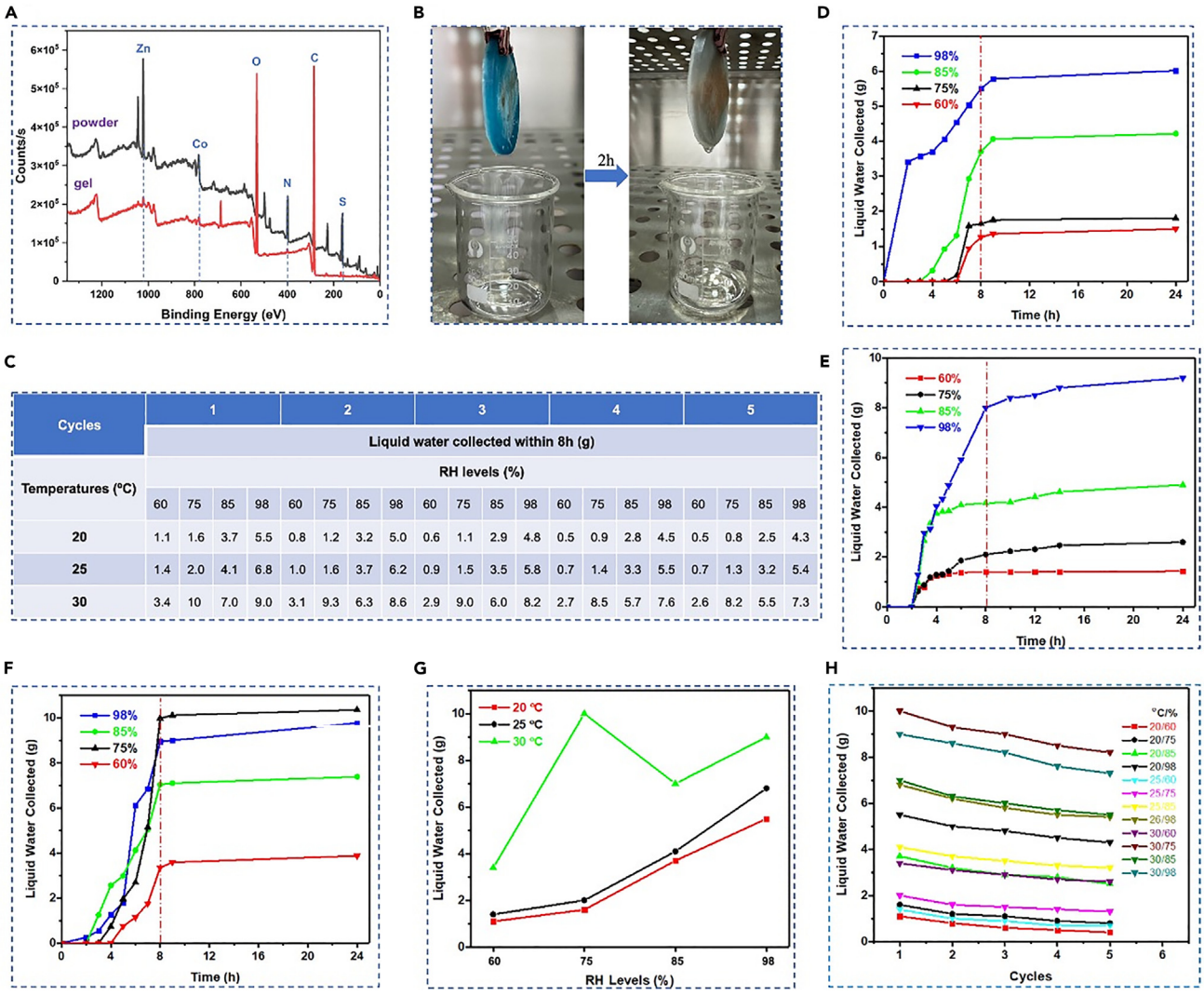

Cycles	1				2				3				4				5			
	Liquid water collected within 8h (g)																			
Temperatures (°C)	RH levels (%)																			
	60	75	85	98	60	75	85	98	60	75	85	98	60	75	85	98	60	75	85	98
20	1.1	1.6	3.7	5.5	0.8	1.2	3.2	5.0	0.6	1.1	2.9	4.8	0.5	0.9	2.8	4.5	0.5	0.8	2.5	4.3
25	1.4	2.0	4.1	6.8	1.0	1.6	3.7	6.2	0.9	1.5	3.5	5.8	0.7	1.4	3.3	5.5	0.7	1.3	3.2	5.4
30	3.4	10	7.0	9.0	3.1	9.3	6.3	8.6	2.9	9.0	6.0	8.2	2.7	8.5	5.7	7.6	2.6	8.2	5.5	7.3

Figure 3. Spontaneous water oozing performance of the soft drain bed

(A) Comparison of the XPS spectra of the hygroscopic powder and hygroscopic gel.

(B) Digital images showing the spontaneous water oozing process of the soft drain bed.

(C) Summary of the amount of liquid water collected in the beaker within 8 h under different RH levels and temperatures during different cycles.

(D) Time-dependent variation of the amount of collected liquid water under 20°C.

(E) Time-dependent variation of the amount of collected liquid water under 25°C.

(F) Time-dependent variation of the amount of collected liquid water under 30°C.

(G) Illustrating the influence of temperature on water oozing ability.

(H) Variation of water oozing ability during different cycles.

remarkable color change; however, no liquid water can be spontaneously oozed during the whole tested temperature range within even 24 h (Figure S3). This phenomenon must be attributed to the adsorption non-saturation of the soft drain bed, as the weight of it was just increased by 19% and 24% with RH levels of 30% and 45%, under 25°C, respectively. When the RH level was increased to 60%, the weight of the soft drain bed increased rapidly by 35% within 2 h; thereafter, continuous drops of freshwater began to drip spontaneously from the drain bed into the beaker (Figure 3B and Video S1). At this moment, the goal of spontaneous water oozing has been achieved on this soft drain bed.

To fully demonstrate its spontaneous water oozing ability and screen out the optimal working condition for the soft drain bed, the incubator was set with different RH levels (60%, 75%, 85%, and 98%) as well as different temperatures (20°C, 25°C, and 30°C). The spontaneous water oozing ability was evaluated by tracking the time-dependent weight variations of the collected liquid water in the beaker, and the corresponding results were summarized in Figures 3C–3F, where the results are found to be both RH level and temperature dependent. On the one hand, the spontaneous water oozing abilities are found to be positively correlated with the temperature (Figure 3G); that is, the higher the temperature, the more excellent the oozing ability. For instance, with the RH level of 98%, the hanging soft drain bed can produce 5.5, 6.8, and

9.0 g freshwater within 8 h, giving an average spontaneous water oozing ability of 0.69, 0.85, and 1.13 g/h under 20°C, 25°C, and 30°C, respectively. This aspect can be ascribed to the less adsorption heat release of the drain bed under higher temperatures that promotes moisture sorption.[43] On the other hand, the correlation between spontaneous water oozing abilities and RH levels is relatively complicated (Figure 3G). To be specific, for relatively lower temperatures of 20°C and 25ºC, the oozing abilities were found to be 0.14, 0.2, and 0.46 g/h and 0.18, 0.25, and 0.51 g/h, for RH levels of 60%, 75%, and 85%, respectively, which are positively correlated with the RH levels. While, for relatively higher temperatures of 30°C, the positive correlation is maladaptive, the oozing abilities were found to be 0.43, 1.25, and 0.88 g/h for RH levels of 60%, 75%, and 85%, respectively. The reason for the superiority of the RH level of 75% can be attributed to the trade-off between the energy and mass flows in the sorption-desorption cycle; that is, under relatively higher temperatures, the higher the RH levels, the higher the specific enthalpy of the vapor that goes against the release of liquid water.[43] These results have suggested that the balance between the temperature and RH level should be a trade-off in considering the practical water oozing application of the present drain bed.

One thing that should be stressed is that, under all tested conditions, the amount of liquid water increased rapidly during the first 8 h, while further extending the exposure time from 8 to 24 h only contributed to a slight increase in liquid water amounts (Figures 3D–3F), suggesting that the optimal working time of the hanging soft drain bed in the in-closed incubator is 8 h. This phenomenon must be attributed to the exothermic characteristic of both the moisture absorption and water oozing process,[44] which has increased the space temperature of the in-closed incubator; as a consequence, the water absorption and liquefaction progress has been hindered. In other words, after 8 h of optimal working time, the drain bed reaches the sorption-desorption saturation, which needs activation for further cycles. The exhausted drain beds were then exposed to the free natural sunlight for 2 h; after that, they repeated the aforementioned 8 h of spontaneous water oozing process. Results show (Figures 3C and 3H) a decrease in oozing ability between the first two cycles; thereafter, the decrease was slowed down. After repeated 5 cycles, the drain bed can reserve approximately 80% of its spontaneous water oozing ability, with the collected freshwater still meeting WHO drinking water standards. Last but not the least, the cost of the soft drain bed is about 0.5 ¥/g, corresponding to the water production cost of 0.275 ¥/g, suggesting the economy, excellent sustainability, and high potential for practical application in decentralized freshwater supply.

Conclusion

In summary, the sustained spontaneous water oozing under all-weather humidity conditions around room temperatures, via energy-free AWH, has been demonstrated on a soft drain bed composed of hydrophilic cloth and hygroscopic gel. Such designation accounts for the effective capture of atmospheric water and is followed by converting it into liquid water spontaneously. Compared with the energy-consuming characteristics of the most conventional even novel synthetic sorbents, the present soft drain bed has achieved direct vapor sorption, liquidation, and liquid water release without condensation, providing a practical strategy for the development of future energy-saving decentralized freshwater supply systems.

Limitations of the study

The RH levels at a specific location can vary throughout the day, affecting the spontaneous water oozing ability of the soft drain bed; assuming an insignificant influence of this factor, we excluded it from our consideration.

STAR★METHODS

Detailed methods are provided in the online version of this paper and include the following:

- KEY RESOURCES TABLE
- RESOURCE AVAILABILITY
  - Lead contact
  - Materials availability
  - Data and code availability
- METHOD DETAILS
  - General considerations
  - Characterizations
  - Preparation of hygroscopic powder [S1]
  - Preparation of hygroscopic gel[S2-S7]
  - Fabrication of the soft drain bed

SUPPLEMENTAL INFORMATION

Supplemental information can be found online at https://doi.org/10.1016/j.isci.2024.110492.

ACKNOWLEDGMENTS

This research was supported by the Jiangsu Provincial Department of Science and Technology Innovation Support Program (no. BK20222004 and BZ2022036) and the Fundamental Research Funds for the Central Universities (no. 2242024K40035).

AUTHOR CONTRIBUTIONS

Y.-H.L.: conceptualization, funding acquisition, supervision, writing – original draft, and writing – review and editing. X.-T.J., M.L., S.-W.S., and J.Z.: investigation.

DECLARATION OF INTERESTS

The authors declare no competing interests.

Received: April 19, 2024
Revised: June 21, 2024
Accepted: July 9, 2024
Published: July 14, 2024

REFERENCES

1. Vörösmarty, C.J., McIntyre, P.B., Gessner, M.O., Dudgeon, D., Prusevich, A., Green, P., Glidden, S., Bunn, S.E., Sullivan, C.A., Liermann, C.R., and Davies, P.M. (2010). Global threats to human water security and river biodiversity. Nature *467*, 555–561.
2. Zhang, L., Xu, Z., Zhao, L., Bhatia, B., Zhong, Y., Gong, S., and Wang, E.N. (2021). Passive, high-efficiency thermally-localized solar desalination. Energy Environ. Sci. *14*, 1771–1793.
3. Elimelech, M., and Phillip, W.A. (2011). The Future of Seawater Desalination: Energy, Technology, and the Environment. Science *333*, 712–717.
4. LaPotin, A., Kim, H., Rao, S.R., and Wang, E.N. (2019). Adsorption-Based Atmospheric Water Harvesting: Impact of Material and Component Properties on System-Level Performance. Acc. Chem. Res. *52*, 1588–1597.
5. Lord, J., Thomas, A., Treat, N., Forkin, M., Bain, R., Dulac, P., Behroozi, C.H., Mamutov, T., Fongheiser, J., Kobilansky, N., et al. (2021). Global potential for harvesting drinking water from air using solar energy. Nature *598*, 611–617.
6. Poredoš, P., Shan, H., Wang, C., Deng, F., and Wang, R. (2022). Sustainable water generation: grand challenges in continuous atmospheric water harvesting. Energy Environ. Sci. *15*, 3223–3235.
7. Fathieh, F., Kalmutzki, M.,J., Kapustin, E.A., Waller, P.J., Yang, J., and Yaghi, O.M. (2018). Practical water production from desert air. Sci. Adv. *4*, eaat3198.
8. Hanikel, N., Pei, X., Chheda, S., Lyu, H., Jeong, W., Sauer, J., Gagliardi, L., and Yaghi, O.M. (2021). Evolution of water structures in metal-organic frameworks for improved atmospheric water harvesting. Science *374*, 454–459.
9. Liu, X., Gao, H., Ward, J.E., Liu, X., Yin, B., Fu, T., Chen, J., Lovley, D.R., and Yao, J. (2020). Power generation from ambient humidity using protein nanowires. Nature *578*, 550–554.
10. Gao, S., and Wang, Z. (2023). Capture fog for clean water. Nat. Sustain. *6*, 1514–1515.
11. Yu, Z., Zhu, T., Zhang, J., Ge, M., Fu, S., and Lai, Y. (2022). Fog Harvesting Devices Inspired from Single to Multiple Creatures: Current Progress and Future Perspective. Adv. Funct. Mater. *32*, 2200359.
12. Yu, Z., Zhang, J., Li, S., Zhou, Z., Qin, Z., Liu, H., Lai, Y., and Fu, S. (2022). Bio-inspired Copper Kirigami Motifs Leading to a 2D–3D Switchable Structure for Programmable Fog Harvesting and Water Retention. Adv. Funct. Mater. *33*, 2210730.
13. de Vega, M., Venegas, M., and García-Hernando, N. (2022). Viability on the desorption and air condensation of water in a compact membrane-based microchannel desorber-condenser for cooling applications. Energy Convers. Manag. *267*, 115919.
14. Zhou, X., Lu, H., Zhao, F., and Yu, G. (2020). Atmospheric Water Harvesting: A Review of Material and Structural Designs. ACS Mater. Lett. *2*, 671–684.
15. Kalmutzki, M.J., Diercks, C.S., and Yaghi, O.M. (2018). Metal-Organic Frameworks for Water Harvesting from Air. Adv. Mater. *30*, e1704304.
16. Ejeian, M., and Wang, R.Z. (2021). Adsorption-based atmospheric water harvesting. Joule *5*, 1678–1703.
17. Meng, Y., Dang, Y., and Suib, S.L. (2022). Materials and devices for atmospheric water harvesting. Cell Rep. Phys. Sci. *3*, 100976.
18. Capri, A., Frazzica, A., and Calabrese, L. (2020). Recent Developments in Coating Technologies for Adsorption Heat Pumps: A Review. Coatings *10*, 855.
19. Feng, Y., Wang, R., and Ge, T. (2022). Pathways to Energy-efficient Water Production from the Atmosphere. Adv. Sci. *9*, e2204508.
20. Batisha, A. (2022). Horizon scanning process to foresight emerging issues in Arabsphere's water vision. Sci. Rep. *12*, 12709.
21. Nguyen, H.L. (2023). Covalent Organic Frameworks for Atmospheric Water Harvesting. Adv. Mater. *35*, e2300018.
22. Fuchs, A., Knechtel, F., Wang, H., Ji, Z., Wuttke, S., Yaghi, O.M., and Ploetz, E. (2023). Water Harvesting at the Single-Crystal Level. J. Am. Chem. Soc. *145*, 14324–14334.
23. Zhang, Z., Fu, H., Li, Z., Huang, J., Xu, Z., Lai, Y., Qian, X., and Zhang, S. (2022). Hydrogel materials for sustainable water resources harvesting & treatment: Synthesis, mechanism and applications. Chem. Eng. J. *439*, 135756.
24. Schweng, P., Mayer, F., Galehdari, D., Weiland, K., and Woodward, R.T. (2023). A Robust and Low-Cost Sulfonated Hypercrosslinked Polymer for Atmospheric Water Harvesting. Small *19*, e2304562.
25. Han, X., Zhong, L., Zhang, L., Zhu, L., Zhou, M., Wang, S., Yu, D., Chen, H., Hou, Y., and Zheng, Y. (2023). Efficient Atmospheric Water Harvesting of Superhydrophilic Photothermic Nanocapsule. Small *19*, 2303358.
26. Deng, F., Chen, Z., Wang, C., Xiang, C., Poredos, P., and Wang, R. (2022). Hygroscopic Porous Polymer for Sorption-Based Atmospheric Water Harvesting. Adv. Sci. *9*, e2204724.
27. Min, X., Wu, Z., Wei, T., Hu, X., Shi, P., Xu, N., Wang, H., Li, J., Zhu, B., and Zhu, J. (2023). High-Yield Atmospheric Water Harvesting Device with Integrated Heating/Cooling Enabled by Thermally Tailored Hydrogel Sorbent. ACS Energy Lett. *8*, 3147–3153.
28. Tao, Y., Li, Q., Wu, Q., and Li, H. (2021). Embedding metal foam into metal-organic framework monoliths for triggering a highly efficient release of adsorbed atmospheric water by localized eddy current heating. Mater. Horiz. *8*, 1439–1445.
29. Huang, Z., Zhang, T., Ju, A., Xu, Z., and Zhao, Y. (2024). Macroporous, Highly Hygroscopic, and Leakage-Free Composites for Efficient Atmospheric Water Harvesting. ACS Appl. Mater. Interfaces *16*, 16893–16902.
30. Cai, C., Chen, Y., Cheng, F., Wei, Z., Zhou, W., and Fu, Y. (2024). Biomimetic Dual Absorption-Adsorption Networked MXene Aerogel-Pump for Integrated Water Harvesting and Power Generation System. ACS Nano *18*, 4376–4387.
31. Shan, H., Zeng, Z., Yang, X., Poredoš, P., Yu, J., Chen, Z., and Wang, R. (2023). Harvesting Thermal Energy and Freshwater from Air through Sorption Thermal Battery Enabled by Polyzwitterionic Gel. ACS Energy Lett. *8*, 5184–5191.
32. Feng, Y., Ge, L., Zhao, Y., Li, Q., Wang, R., and Ge, T. (2024). Active MOF water harvester with extraordinary productivity enabled by cooling-enhanced sorption. Energy Environ. Sci. *17*, 1083–1094.
33. Hanikel, N., Prevot, M.S., and Yaghi, O.M. (2020). MOF water harvesters. Nat. Nanotechnol. *15*, 348–355.
34. (2023). Converting air moisture into water. Nature Water *1*, 563.
35. Ghosh, R., Baut, A., Belleri, G., Kappl, M., Butt, H.-J., and Schutzius, T.M. (2023). Photocatalytically reactive surfaces for simultaneous water harvesting and treatment. Nat. Sustain. *6*, 1663–1672.
36. Zhang, L., Fang, W.-X., Wang, C., Dong, H., Ma, S.-H., and Luo, Y.-H. (2021). Porous frameworks for effective water adsorption: from 3D bulk to 2D nanosheets. Inorg. Chem. Front. *8*, 898–913.
37. Guidelines for Drinking-Water Quality: Fourth Edition Incorporating the First and Second Addenda, Geneva (2022 (Switzerland: World Health Organization).
38. Luo, Y.-H., Wang, C., Ma, S.-H., Jin, X.-W., Zou, Y.-C., Xu, K.-X., Fang, W.-X., Zhang, L., and Dong, H. (2021). Humidity reduction by using hetero-layered metal-organic

framework nanosheet composites as hygroscopic materials. Environ. Sci. Nano *8*, 3665–3672.

39. Xue, C., Zhang, S.X., Zeng, F.L., Dong, H., Ma, S.H., and Luo, Y.H. (2023). In Situ All-Weather Humidity Visualization by Using a Hydrophilic Sponge. Adv. Mater. Technol. *8*, 2201188.
40. Liu, M., Ma, S.H., Dong, H., Zeng, F.L., Jin, X.T., and Luo, Y.H. (2023). Rewritable Paper Based on Layered Metal-Organic Frameworks with NIR-Triggered Reversible Color Switching. Adv. Opt. Mater. *11*, 2300056.
41. Zhang, Y., Wu, L., Wang, X., Yu, J., and Ding, B. (2020). Super hygroscopic nanofibrous membrane-based moisture pump for solar-driven indoor dehumidification. Nat. Commun. *11*, 3302.
42. Song, Y., Xu, N., Liu, G., Qi, H., Zhao, W., Zhu, B., Zhou, L., and Zhu, J. (2022). High-yield solar-driven atmospheric water harvesting of metal-organic- framework-derived nanoporous carbon with fast-diffusion water channels. Nat. Nanotechnol. *17*, 857–863.
43. Tan, K.T., Tao, S., Huang, N., and Jiang, D. (2021). Water cluster in hydrophobic crystalline porous covalent organic frameworks. Nat. Commun. *12*, 6747.
44. Entezari, A., Esan, O.C., Yan, X., Wang, R., and An, L. (2023). Sorption-Based Atmospheric Water Harvesting: Materials, Components, Systems, and Applications. Adv. Mater. *35*, e2210957.

STAR★METHODS

KEY RESOURCES TABLE

REAGENT or RESOURCE	SOURCE	IDENTIFIER
Polyethylene glycol (PEG-6000, 99%)	Macklin	25322-68-3
Dimethylacetamide (DMF, 99.9%)	Macklin	68-12-2
Polyvinylidene fluoride (PVDF, 99%)	Aladdin	24937-79-9
Cobalt(II)Thiocyanate ($Co(SCN)_2$, 99%)	Macklin	
Pyrazine ($C_4H_4N_2$, 99%)	Macklin	290-37-9
Acetone (CH_3COCH_3, 99.5%)	Aladdin	67-64-1
Methanol (CH_3OH, 99.9%)	Aladdin	67-56-1
Ammonium thiocyanate (NH_4SCN, 97.5%)	Macklin	1762-95-4
Zinc sulfate Heptahydrate ($ZnSO_4 \cdot 7H_2O$, 99%)	Aladdin	7446-20-0
hydrophilic cloth	Atmospheric Water Research Center (Qiandao Lake, Hangzhou, China)	

RESOURCE AVAILABILITY

Lead contact

Further information and requests for resources and materials should be directed to and will be fulfilled by the lead contact, Yang-Hui Luo (luoyh2016@seu.edu.cn).

Materials availability

This study did not generate new unique reagents. All materials generated in this work are available from the lead contact upon request.

Data and code availability

- The datasets generated in this study are available from the lead contact upon request.
- This work does not report the original code.
- Any additional information required to reanalyze the data reported in this paper can be obtained from the lead contact upon request.

METHOD DETAILS

General considerations

All syntheses were performed under ambient conditions and all the chemicals were of analytical grade and were used without further purification. All the chemicals and all the solvents were purchased from Shanghai MacLean's Biochemical Technology Co. Ltd and Jiu Ding Chemical Technology Co. Ltd. Hydrophobic cloth provided by was provided by the Atmospheric Water Research Center (Qiandao Lake, Hangzhou, China).

Characterizations

The morphologies of hydrophobic cloth, hygroscopic gel, and the soft drain bed were determined by using a field emission scanning electron microscope (SEM; Hitachi S-4800 20 kV). Vapor sorption isotherms of hygroscopic powder were measured by vacuum static gravimetric method with a BSD-VVS system. X-ray photoelectron spectroscopy (XPS) of both the hygroscopic powder and hygroscopic gel was acquired by using a Thermo Scientific K-α+ spectrometer.

Preparation of hygroscopic powder [S1]

Step 1

Synthesis of $Co(NCS)_2(pyrazine)_2$. $Co(SCN)_2$ (1.736 g) was added to a deionized water solution (40 mL) at room temperature under atmospheric pressure. After that, the obtained mixtures were ultrasonic until the sample had been completely dissolved to get a transparent solution. Then, the above suspension was added slowly at a rate of two drops per second under stirring to an acetone solution (130 mL) containing pyrazine (1.82 g). In the process of adding, the color of the solution gradually changed from red to purple at first. After continued dripping, it appeared grayish-green and eventually brick-red. Finally, $Co(NCS)_2(pyrazine)_2$ was collected via vacuum filtration before drying by vacuum overnight.

Step 2

Synthesis of $Zn(NCS)_2(pyrazine)_2$. pyrazine (0.8808 g) was dissolved in 40 mL of methanol solution, then $ZnSO_4 \cdot 7H_2O$ (2.876 g) was dissolved in 40 mL of methanol solution and added to the above pyrazine solution, placed on a magnetic stirrer, the solution became white and turbid. Then, NH_4SCN (3.044 g) was dissolved in 45 mL of methanol solution and added to the above-mixed solution. After stirring for 1 h, the resulting mixture was under filtration, and vacuum dried to get $Zn(NCS)_2$ $(pyrazine)_2$.

Step 3

$Co(NCS)_2(pyrazine)_2$ (0.3 g) and $Zn(NCS)_2(pyrazine)_2$ (0.3 g) were added to anhydrous ethanol (500 mL) and ultrasonicated for 1 h respectively. The obvious Tyndall effect was observed by irradiating the solution with a laser pointer. After that, the above two suspensions were mixed at a 1:1 volume ratio, the mixed solution was magnetically stirred overnight, and finally, rotary evaporation was done to obtain the 2D hygroscopic powder.

Preparation of hygroscopic gel[S2-S7]

Polyethylene glycol-6000 (1.35 g) was dissolved in 45 mL N, N-dimethyl-formamide, and the solution was ultrasonicated until it became clear. Afterward, poly (vinylidene-fluoride) (3.60 g) was added slowly, followed by stirring for 1 h. Then 0.05 g of 2D hygroscopic powder was gradually added to the above mixtures. After stirring for 1 h, the resulting suspension was then transferred to an oil bath at 90°C under continuous magnetic stirring for 6 h. Finally, the target product was formed by cooling to room temperature.

Fabrication of the soft drain bed

To fabricate the soft drain bed, the hygroscopic gel was first prepared, and then injected into a circular mold under 90°C, after that, the hydrophilic cloth was immersed and suspended in the middle part of the roving hygroscopic gel. The obtained mixtures were then standing under 90°C for 1 h, which was then followed by cooling to room temperature to get the target soft drain bed.